Bcl-2 is the target of a UV-inducible apoptosis switch and a node for UV signaling

Dejan Knezevic*†‡, Wengeng Zhang*, Patrick J. Rochette*, and Douglas E. Brash*§¶‖

Departments of *Therapeutic Radiology, §Genetics, ¶Dermatology, and †Physiology, Yale University School of Medicine, 333 Cedar Street, New Haven, CT 06525

Edited by Richard B. Setlow, Brookhaven National Laboratory, Upton, NY, and approved May 19, 2007 (received for review February 12, 2007)

Sunlight's UVB radiation triggers cell signaling at multiple sites to induce apoptosis. The integration of these signal entry sites is not understood. Here we show that P53 and E2f1 constitute a UV-inducible apoptosis switch. At low-UV doses, wild-type cells resemble the OFF state of an siP53-treated cell, whereas at high-UV doses, the apoptosis frequency transitions to the fully ON behavior of an siE2f1-treated cell. The switch's target is Bcl-2: Rapid Bcl-2 down-regulation in response to UVB-induced DNA photoproducts is lost in P53-deficient cells, but, as for apoptosis, is restored when both P53 and its inhibited target E2f1 are absent. P53's down-regulation of Bcl-2 is mediated entirely through E2f1. Bcl-2 is also down-regulated by a separate pathway triggered by DNA photoproducts in the absence of P53 and E2f1. Four UV pathways terminating on Bcl-2 contribute to apoptosis after UVB irradiation. The apoptosis lost in $p53^{-/-}$ is completely restored by siBcl-2, implying that Bcl-2 is a rate-limiting member of this network. These results identify Bcl-2 as an integrator of several UV-induced proapoptotic signals and show that it, in turn, suppresses a direct UV–apoptosis pathway. UV-induced apoptosis requires both UV activation of the direct pathway and a separate UV disinhibition of this pathway through P53–E2f1–Bcl-2.

E2f1 | P53 | stress response | network | systems biology

The apoptotic activity of P53, a transcription factor frequently mutated in tumors, has been considered to stem from its transcriptional activation of genes for Bax, Bak, PUMA, and PIGs, as well as directly binding antiapoptotic proteins at the mitochondria (1, 2). However, we and others discovered that, for UV radiation, inactivating E2f1 restores wild-type levels of UVB-induced apoptosis to $p53^{-/-}$ cells (3, 4). This result implicates an underlying direct apoptosis pathway that is separately activated by UVB and is *p53*-independent in the sense of being active in a *p53* knockout cell (provided E2f1 is also absent). Yet the flow through this pathway is modulated by a P53–E2f1 apoptosis switch. The direct pathway may have other important activities because some *E2f1* knockout constructs restore low cancer and birth defect frequencies to *p53*-deficient mice (3). Two questions arise: Does UV-induced P53 dial up this apoptosis switch by converting it to an $E2f1^{-/-}$-like ON state? What target of E2f1 then connects this switch to the direct apoptosis pathway?

E2f1 is a transcription factor that acts at the G_1–S transition, but also has a proapoptotic function when it is highly overexpressed in cells starved of growth factors (5–7). It up-regulates proapoptotic P73, Bid, and Apaf-1; inhibits antiapoptotic Mcl-1; and is part of the DNA damage response (8). Many of these effects are *p53*-dependent, seemingly placing P53 downstream of E2f1 (7, 9). Yet UV-induced apoptosis *in vivo* or in unstarved primary cells (*i*) uses an antiapoptotic activity of E2f1 that lies downstream of P53, and (*ii*) proceeds normally in E2f1 knockout cells (3). P53 and E2f1 in fact form a feedback loop in which individual proteins are difficult to characterize as up- or downstream, pro- or antiapoptotic (10). Proapoptotically, E2f1 up-regulates P53 through the Arf–Mdm2 pathway. However, P53 also suppresses downstream E2f1: It up-regulates P21, thereby dephosphorylating Rb and allowing it to bind up free E2f1; it displaces DP1 from E2f1 (11), and it up-regulates Mdm2, which targets E2f1 for ubiquitination (12). Antiapoptotically, E2f1 up-regulates proteins such as Bcl-2 and inhibits transcription of proapoptotic proteins such as Fas (10, 13). Antiapoptotic E2f1 is also seen in *Drosophila* development.

To understand this network, we used RNAi and single- and double-knockout strains to identify proteins whose UV-induced proapoptotic behavior was (*i*) lost in $p53^{-/-}$ cells, and (*ii*) restored to wild-type levels by subsequent E2f1 inactivation in $p53^{-/-}$;$E2f1^{-/-}$ cells. Primary fibroblasts were used, rather than tumor-derived cell lines, to avoid abnormal cell cycle and signal transduction pathways.

Results

Single-Genotype *in Vitro* System. To rule out the possibility that the antiapoptotic function of E2f1 relies on particular knockout constructs or genetic background, we established an RNAi-based system in a single genotype. Primary wild-type mouse skin fibroblasts were transfected with noncoding control RNAi, siP53, or siE2f1. These siRNAs efficiently suppressed their intended targets (Fig. 1*A Inset*). Next, wild-type cells were transfected with noncoding siRNA (for wild-type fibroblasts) and $p53^{-/-}$ cells with either siP53 (negative control) or siE2f1. Thirty-six hours later, transfected cells were irradiated with 0 or 750 J/m^2 UVB, and 20 h later the percentage of apoptotic cells was measured by the Annexin V assay. Nonirradiated cells of all three groups had few apoptotic cells (≈4%), and the groups were statistically indistinguishable. Only a fraction of irradiated cells undergo apoptosis because S-phase is also required (14–16) and the UVB dose corresponds to a modest beach exposure. UVB-irradiated $p53^{-/-}$ cells had 5-fold fewer apoptotic cells than wild type (Fig. 1*A*) due to the P53 dependence of UVB-induced apoptosis (17). Transfecting $p53^{-/-}$ cells with siE2f1 restored apoptosis to the wild-type level. This RNAi result reproduces the *in vivo* and *in vitro* results seen with double-knockout cells (3), implying that the antiapoptotic function of E2f1 is an inherent function of the protein.

P53 and E2f1 Act as a UV-Inducible Switch. To determine how UV-induced P53 protein controls the behavior of the P53/E2f1 regulatory network, we compared the dose–response of apoptosis in wild-type fibroblasts to that in cells treated with RNAi. siP53 establishes the fully OFF behavior of a cell missing P53; siE2f1 establishes the fully ON behavior of the direct apoptosis pathway without its P53–E2f1 regulator.

At a low dose at which P53 was not detectably induced (250

Author contributions: D.K. and D.E.B. designed research; D.K., W.Z., and P.J.R. performed research; and D.K. and D.E.B. wrote the paper.

The authors declare no conflict of interest.

This article is a PNAS Direct Submission.

‡Present address: Genentech, Inc., Research Pathology, 1 DNA Way, South San Francisco, CA 94080.

‖To whom correspondence should be addressed. E-mail: douglas.brash@yale.edu.

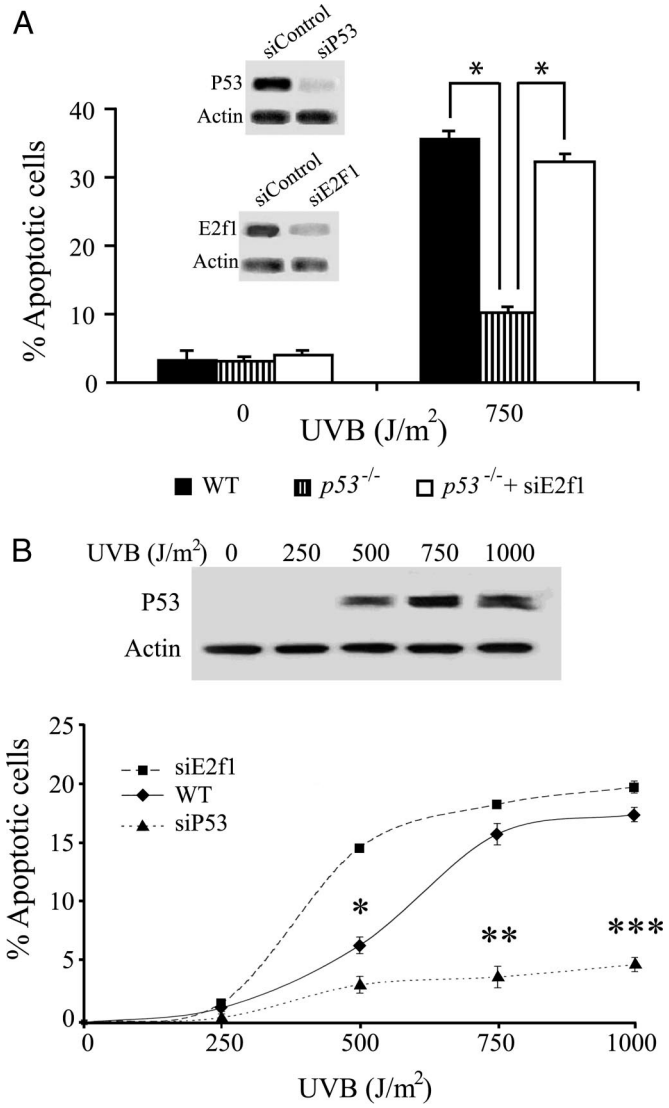

Fig. 1. P53 regulates UV-induced apoptosis through E2f1 in isogenic cells. (*A*) E2f1 RNAi restores apoptosis to $p53^{-/-}$ fibroblasts. (*Inset*) Western blots of wild-type cells treated with (*Upper*) 100 nM siControl nontargeting RNAi or 100 nM siP53 or (*Lower*) 100 nM siE2f1. Histogram: Primary $p53^{-/-}$ fibroblasts treated with 100 nM siE2f1 or control siP53. Twenty hours after irradiation, apoptosis was measured by using AnnexinV. Each bar represents three independent experiments using cells derived from seven mice. Apoptosis is reduced 4-fold in UVB-irradiated $p53^{-/-}$ cells and restored with siE2f1. The difference between irradiated $p53^{-/-}$ fibroblasts and WT, or after siE2f1 treatment, is statistically significant (*, $P = 0.005$). (*B*) P53 and E2f1 behave as a UV-inducible switch. (*Lower*) Wild-type (WT) cells treated with control nontargeting RNAi, siE2f1, or siP53 were irradiated with increasing doses of UVB. Apoptosis was measured 20 h later. Each point represents an average of two experiments from cells from five mice. At a low dose (250 J/m^2), the percentage of apoptotic cells is indistinguishable between genotypes ($P = 0.15$ for WT vs. siE2f1; $P = 0.07$ for siE2f1 vs. siP53). At an intermediate dose (500 J/m^2), WT differs from both siE2f1 (*, $P = 0.01$) and siP53 (*, $P = 0.02$). In contrast, at high doses, where P53 is activated (750 and 1,000 J/m^2), WT's behavior resembles that of the siE2f1 fully ON state ($P = 0.11$; $P = 0.12$), and the difference from siP53 is significant (**, $P = 0.002$; ***, $P = 0.001$, respectively). (*Upper*) Western blot of P53 protein induced in wild-type cells 24 h after the same UVB doses.

J/m^2), the percentage of apoptotic cells was indistinguishable in the three genotypes (Fig. 1*B Lower*). At an intermediate dose (500 J/m^2), wild type differed from both siE2f1 and siP53 samples in an apparent transition from fully OFF to fully ON states. At the two highest doses, the behavior of the wild-type cells resembled that of the siE2f1 fully ON state. This UV-induced switch in behavior corresponds to the circuit in which E2f1 inhibits a UV-induced apoptosis pathway and UV-induced P53 activates apoptosis by inhibiting the inhibitor (3).

P53 and E2f1 Regulate Bcl-2. To identify the pathway suppressed by E2f1, we used immunoblotting to assay major pro- and antiapoptotic proteins, including those known to be regulated by E2f1. Proteins were sought whose UVB-induced expression was altered by loss of P53 and restored to normal by additional loss of E2f1. Fas, FasL, TNFα, and P73 were not detectable. Jnk1 and Jnk 2 are required for UV-induced apoptosis (18), but were unaffected by P53. UV induction of proapoptotic Bax and Bak, and degradation of antiapoptotic Bcl-xL, were P53-dependent, but were unaffected by E2f1. The P53–E2f1 apoptosis switch therefore does not operate through these proteins.

In contrast, the antiapoptotic protein Bcl-2 fit the anticipated pattern. Bcl-2 suppresses a critical point in the mitochondrial pathway of apoptosis, the release of cytochrome *c* from the intermembrane space. It is thought to act by inhibiting the conformational change or oligomerization of the proapoptotic proteins Bax and Bak at lipid pores (2). UVB irradiation causes a rapid decline of Bcl-2, due primarily to ubiquitination and subsequent proteasomal degradation (19–21). In our hands, this decline was 5-fold in wild-type cells at passage level 5 or lower (Fig. 2*A*). The response was slower at higher passages. The UVB-induced decline was completely abolished in $p53^{-/-}$ cells, but was restored in the $p53^{-/-}$;$E2f1^{-/-}$ double knockout (Fig. 2*A*). The decline was also largely abolished in the $E2f1^{-/-}$ single knockout (Fig. 2*A*; see also control lanes in Fig. 2*D*), implying that UV's down-regulation of Bcl-2 is mediated primarily through E2f1. (Why the double knockout nevertheless restores the Bcl-2 decline, allowing UV to induce apoptosis in $E2f1^{-/-}$, becomes clear later.) We conclude that Bcl-2, like UV-induced apoptosis in wild-type cells, is regulated by P53's inhibition of E2f1.

Basal expression of Bcl-2 was also E2f1-dependent (Fig. 2*A*, 0 UV gel lanes and histogram bars). Inactivating E2f1 in a wild-type background ($E2f1^{-/-}$) or in a $p53^{-/-}$ background ($p53^{-/-}$;$E2f1^{-/-}$) reduced the basal level of Bcl-2 by ≈60%. To confirm that basal Bcl-2 is regulated by E2f1, we transfected 4 μg of empty pcDNA3.1 vector or pcDNA3.1-E2F1 vector expressing human E2F1 into primary $p53^{-/-}$;$E2f1^{-/-}$ mouse fibroblasts. The E2F1 vector caused a 4-fold up-regulation of basal Bcl-2 protein (Fig. 2*B Inset*). Conversely, siE2f1 decreased basal Bcl-2 (Fig. 2*B*). Transfected P53 was able to suppress Bcl-2 only when E2f1 was present (Fig. 2*C*). Indeed, the low levels of basal Bcl-2 in $E2f1^{-/-}$ cells were actually increased slightly by *p53* (Fig. 2*C Right*; see also Fig. 2*D*, 0 UV).

We next tested directly whether UV-induced P53 suppresses E2f1's up-regulation of Bcl-2. Increasing amounts of E2F1 vector were transfected into E2f1-defective cells that either lacked P53 ($p53^{-/-}$;$E2f1^{-/-}$) or contained wild-type P53 ($p53^{+/+}$;$E2f1^{-/-}$). In the absence of P53, increased E2F1 vector led to increased amounts of Bcl-2 protein in UVB-irradiated cells (Fig. 2*D Right*). When P53 was present, however, E2F1 transfection did not elevate Bcl-2 (Fig. 2*D Left*), indicating that P53 prevents E2f1 from activating Bcl-2. This pattern of Bcl-2 expression resembles the behavior of the P53–E2f1 switch in apoptosis (3). It implies that Bcl-2 is a downstream target of E2f1 and both proteins are functionally downstream of P53. (The origin of the residual UV-induced Bcl-2 decrease in $E2f1^{-/-}$ cells becomes clear later.)

Bcl-2 Is the Key Regulator of the Direct UV-Induced Apoptosis Pathway. Bcl-2 is already known to be important in the P53–Bax–Bak pathway of apoptosis (2). However, many proteins contribute to apoptosis, including direct transcriptional targets of P53 [Bax,

CELL BIOLOGY

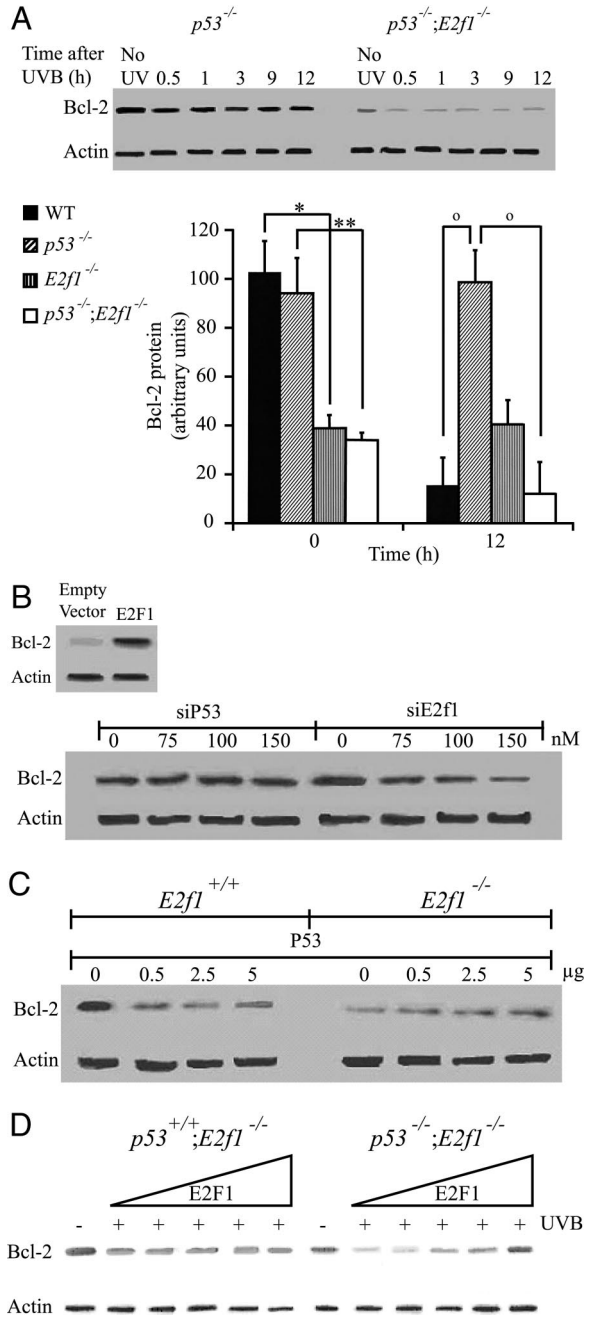

Fig. 2. E2f1 regulates UVB-induced and basal levels of Bcl-2. (*A*) The E2f1 knockout restores the ability of $p53^{-/-}$ cells to down-regulate Bcl-2 after UVB. (*Lower*) $p53^{-/-}$ and $p53^{-/-}$;$E2f1^{-/-}$ primary fibroblasts were irradiated with 1,000 J/m^2 UVB, and 11 μg of protein from each time point was electrophoresed and blotted by using Bcl-2 antibody (sc-7382; Santa Cruz Biotechnology, Santa Cruz, CA) at a 1:100 dilution. (*Upper*) One of four independent Western blots. The 0 UV gel lanes and histogram bars show that E2f1 also up-regulates basal Bcl-2. (*B*) (*Upper*) E2f1 overexpression up-regulates basal Bcl-2. Five micrograms human E2F1 vector pcDNA3.1-E2F1 was transfected into double-knockout ($p53^{-/-}$;$E2f1^{-/-}$) fibroblasts. As control, 5 μg of empty vector (pcDNA3.1) was used. Cells were incubated for 48 h, and Bcl-2 protein expression was visualized by immunoblot. (*Lower*) E2f1 RNAi decreases basal Bcl-2. Increasing amounts of siE2f1 were transfected into $p53^{-/-}$ fibroblasts up to 150 nM (which suppressed E2f1 by 90%). As negative control, siP53 was transfected at the same concentrations. Shown is one of three experiments with similar results. The points with 100 and 150 nM siE2f1 are reduced compared with the control siP53 ($P = 0.03$ and $P = 0.02$, respectively). (*C*) P53 suppresses basal Bcl-2 only when E2f1 is present. Increasing amounts of human *p53* expression vector pCMV-p53 were transfected into wild-type cells or cells derived from $E2f1^{-/-}$ mice. Transfected cells were incubated for 48 h, and the expression of Bcl-2 was visualized by immunoblotting. Shown is one of three similar experiments. In $E2f1^{+/+}$ cells, *p53* decreased basal Bcl-2 levels; the difference from no-*p53* was statistically significant for all points containing exogenous *p53* ($P < 0.05$). In $E2f1^{-/-}$ cells, *p53* actually increased Bcl-2 slightly. (*D*) UV-induced P53 suppresses E2f1's up-regulation of Bcl-2. $E2f1^{-/-}$ and $p53^{-/-}$;$E2f1^{-/-}$ primary fibroblasts were transfected with 0, 0.5, 1, 2.5, and 5 μg of pcDNA3.1-E2F1 vector, adding empty vector to keep transfected DNA at 6 μg. Thirty-six hours later, the cells were irradiated with 750 J/m^2 UVB, and 24 h later the cells were analyzed for Bcl-2 expression with antibody at 1:200 dilution. In the absence of P53 (*Right*), E2F1 up-regulates Bcl-2 after UVB irradiation; P53 prevents this up-regulation and actually causes a net down-regulation after UVB (*Left*).

Bak, Puma, PIGs, Noxa (22)] or E2f1 (P73, Apaf-1, caspase-7), therefore it was important to determine whether Bcl-2 is rate-limiting for the direct UV-apoptosis pathway. We asked how much of the direct pathway could be turned off by Bcl-2. Increasing amounts of Bcl-2 expression vector were transfected into $p53^{-/-}$;$E2f1^{-/-}$ primary fibroblasts. At the highest concentration, 80% of UVB apoptosis in the double knockout was suppressed (Fig. 3*A*). This result indicates that the majority of UVB-induced apoptosis in the direct pathway is regulatable through Bcl-2 and, thus, regulatable by the optional P53–E2f1 apparatus.

It was still possible that Bcl-2 was one of several redundant UV-responsive proteins able to suppress the direct apoptosis pathway. Therefore, we asked the converse question: If the direct apoptosis pathway has been suppressed by a *p53* knockout, how far can it be turned on again by suppressing Bcl-2? If Bcl-2 is a rate-limiting regulator of the direct pathway, the apoptosis defect in P53-deficient cells would be reversed not only by inactivating E2f1, but also by inactivating E2f1's downstream target, Bcl-2. Because the P53→Puma–Noxa–PIGs–Bax–Bak pathway has been removed in $p53^{-/-}$ cells, this experiment tests the direct UVB apoptosis pathway in isolation. Inactivating Bcl-2 completely restored UV-induced apoptosis to $p53^{-/-}$ cells, and the UVB dose–response now resembled that of wild-type cells (Fig. 3*B*). Thus, the direct UVB apoptosis pathway's regulation by P53–E2f1 occurs primarily through Bcl-2. Because UVB did induce apoptosis in the *p53* knockout when Bcl-2 was absent, Bcl-2 still lies outside the direct pathway, rather than being one of the steps within it.

DNA Is the Photoreceptor for a Second Bcl-2 Signaling Pathway. More than 90% of the signal for UVB-induced P53 induction, Mdm2 degradation, and apoptosis in normal cells requires unrepaired DNA photoproducts (23), as does the majority of the signal for Bcl-2 degradation (19, 21). We inquired whether these DNA photoproducts operate solely through P53 and E2f1. Because the signal for Bcl-2 reduction was rapid (Fig. 2*A*), we avoided the usual strategy of testing mutants defective in DNA excision repair: Even wild-type cells would show little repair during this time. Instead, we introduced the enzyme photolyase, which specifically monomerizes cyclobutane pyrimidine dimers in DNA when the bound enzyme is activated by UV wavelengths that do not appreciably induce pyrimidine photoproducts (24). Because the rate-limiting step is the slow binding of photolyase to cyclobutane dimers, photoreactivation may be partial for a fast biological process. A 1-h binding period after UVB led to a 70% reduction in cyclobutane dimers (25). To accommodate the rapid Bcl-2 response, we limited binding and photoreactivation to 5 min.

Surprisingly, photolyase suppressed Bcl-2 degradation in double-knockout cells for at least 12 h, after which degradation proceeded (Fig. 4*A*). Similarly, 60% of the UVB-induced apoptosis at 20 h was prevented by prior brief photolyase treatment

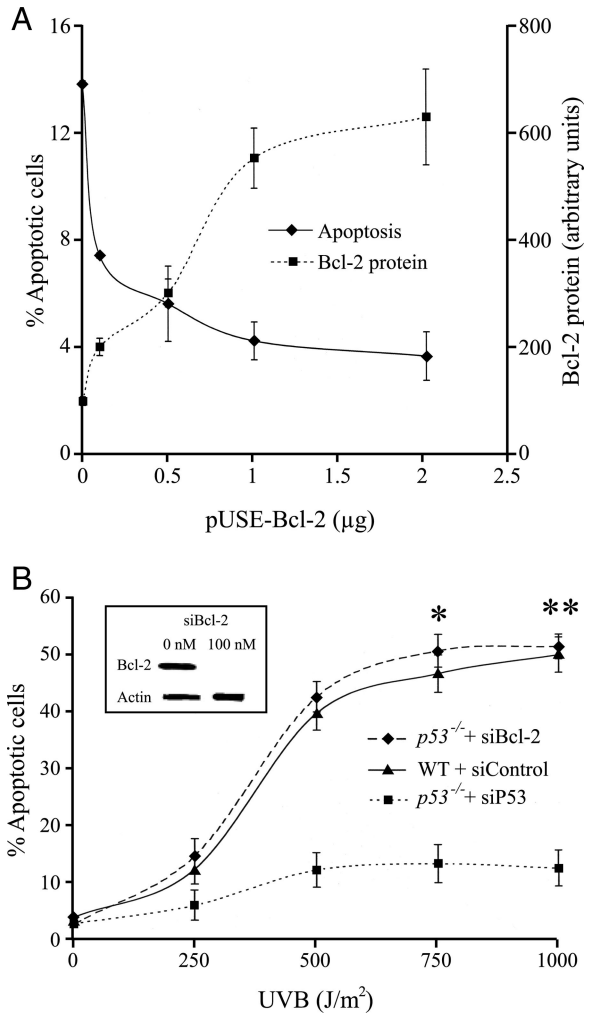

Fig. 3. Bcl-2 is the principal target through which P53 and E2f1 regulate UV-induced apoptosis. (*A*) Exogenous Bcl-2 suppresses most UVB-induced apoptosis in the direct pathway. Increasing amounts of vector pUSE–Bcl-2 (Upstate Biotechnology, Lake Placid, NY) were transfected into $p53^{-/-}$;$E2f1^{-/-}$ fibroblasts by using empty vector to keep total DNA at 2 μg. Transfected cells were incubated for 48 h and irradiated at 500 J/m^2. Twenty hours later, apoptosis was measured by AnnexinV. Each point represents an average of three separate experiments using cells from 10 mice. The differences in apoptosis compared with the 0 *Bcl-2* point were significant ($P = 0.0004$, 0.04, 0.04, and 0.02 for the four *Bcl-2* vector concentrations, respectively). (*B*) Bcl-2 RNAi restores apoptosis to $p53^{-/-}$ fibroblasts. $p53^{-/-}$ primary fibroblasts were transfected with 100 nM siP53 as negative control or with 100 nM siBcl-2. As positive control, wild-type cells were transfected with 100 nM noncoding RNAi. Samples were UVB irradiated, and apoptosis was measured 20 h later. Each point represents three independent experiments using cells derived from 11 mice. The differences at 750 and 1,000 J/m^2 between $p53^{-/-}$ plus siP53 and either wild type plus siControl or $p53^{-/-}$ plus siBcl-2 are statistically significant (*, $P = 0.04$; **, $P = 0.03$). In wild-type cells, siBcl-2 had no effect (data not shown), indicating that the rapid UV down-regulation of Bcl-2 by P53 already achieves maximum apoptosis.

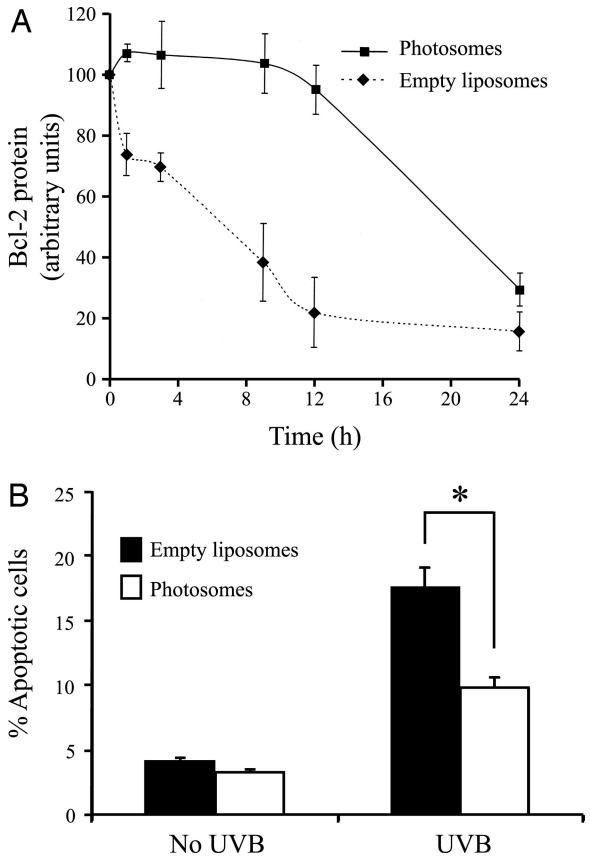

Fig. 4. A second DNA damage signal input to Bcl-2. (*A*) Degradation of Bcl-2 protein in $p53^{-/-}$;$E2f1^{-/-}$ is prevented by repairing cyclobutane pyrimidine dimers after UVB. Cells were pretreated for 1 h with 150 μl of photolyase in liposomes or empty liposomes. Both sets were irradiated with 750 J/m^2 UVB and illuminated with UVA for 5 min to activate the photolyase- and monomerize-bound cyclobutane pyrimidine dimers in DNA, and blots were analyzed for Bcl-2 protein. Each point represents an average of three independent experiments on cells from seven mice. The two treatments are statistically different at 1, 3, 9, and 12 h ($P = 0.04$, 0.04, 0.04, and 0.02, respectively). (*B*) Photolyase suppresses UVB-induced apoptosis in $p53^{-/-}$;$E2f1^{-/-}$ fibroblasts. Cells were treated with photolyase, UVB, and UVA as before and incubated for 20 h, and apoptosis was measured. Each bar represents an average of three repeats with cells from 10 mice. The samples are statistically different (*, $P = 0.04$).

(Fig. 4*B*). The dose–response for UVB-induced apoptosis indicates that this reduction in apoptosis corresponds to an ≈60% reduction in the UV-inducing signal. We conclude that even when the P53–E2f1 regulatory mechanism is absent, a second signaling pathway triggered by cyclobutane pyrimidine dimers in DNA down-regulates Bcl-2 and facilitates apoptosis. This pathway is not the direct pathway because the siBcl-2 experiment showed that the direct pathway lies below Bcl-2 (Fig. 3*B*). Because the *p53* knockout almost completely blocked Bcl-2 degradation after UVB (Fig. 2*A*), the new pathway is evidently a smaller component of the UV response than the P53–E2f1 pathway. It becomes significant in E2f1-defective cells, which have low basal levels of Bcl-2 (Fig. 2*D*, ± UV lanes with no added E2f1). Combining photolyase and siBcl-2 was not possible for technical reasons, leaving open the identity of the photoreceptor for the direct UV-induced apoptosis pathway.

Discussion

A UV-Induced Apoptosis Switch. One tends to think of signal transduction pathways as on or off, but input signals arrive in a range of doses. The present experiments show the behavior of a UV-inducible apoptosis switch. First, UV induces a transition from a fully OFF state (resembling a P53-defective cell) to a fully ON state (resembling an E2f1-defective cell). Intermediate doses result in intermediate behavior (Fig. 1*B*). UV does this by activating P53's inhibition of E2f1's apoptosis-inhibitory activity (Fig. 1*A*). Second, the previously unknown downstream target of this switch is Bcl-2, an apoptosis inhibitor that is activated by E2f1 (Fig. 2). Third, the P53-E2f1 switch and its Bcl-2 target are

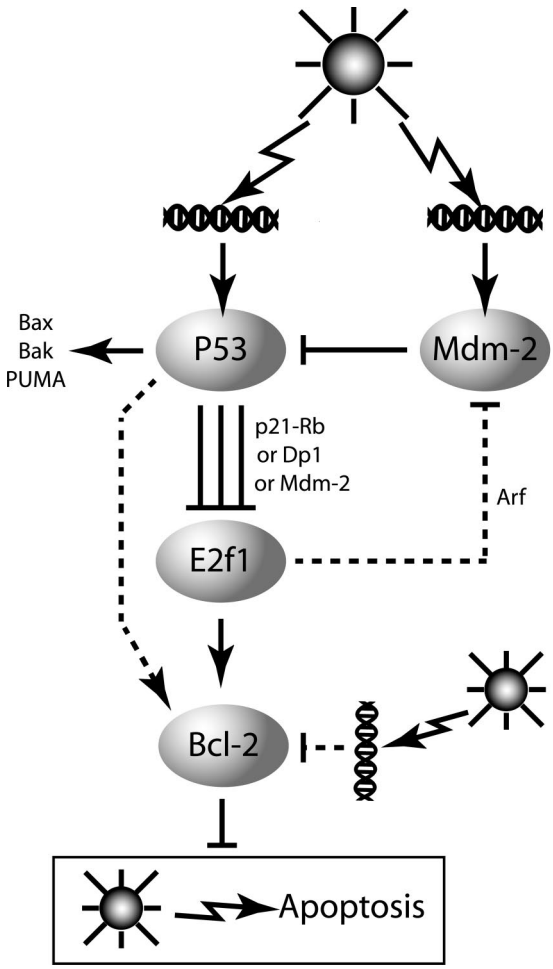

Fig. 5. UVB acts at both the switch and the switched pathway to trigger UV-induced apoptosis. DNA photoproducts trigger phosphorylation of P53 and Mdm2, thereby reducing P53 degradation. In many systems, the elevated P53 triggers apoptosis by transcriptionally activating Bax, Bak, Puma, PIGs, and Noxa, as well as acting directly at mitochondria. For UVB-induced apoptosis, however, a larger signal proceeds through a pathway in which UV-induced P53 inactivates E2f1, as described in the text. Graded doses of UV cause the P53–E2f1 regulatory apparatus to transition from a fully OFF $p53^{-/-}$-like state to a fully ON $E2f1^{-/-}$-like state. The apoptosis-inhibitory activity of E2f1 acts through Bcl-2, which suppresses the information flow in a direct pathway that is triggered by UV even when the P53–E2f1 regulatory apparatus is removed. P53 disinhibits this pathway. Two secondary signaling pathways (dotted lines) are appreciable when basal Bcl-2 is low, as described in the text.

an optional regulatory apparatus sitting atop a direct UV-induced apoptosis pathway that induces apoptosis even in the absence of the switch (Figs. 2 and 3). This direct pathway is normally suppressed by E2f1–Bcl-2. UV-induced P53 removes this suppression, permitting the unfettered action of the UV-activated direct pathway (summarized in Fig. 5). Fourth, the direct pathway is not optional: In the absence of P53 and E2f1, or of Bcl-2, UV is still required for apoptosis (Figs. 1*A* and 3*B*). The direct pathway is therefore P53-nonreliant but P53-modulatable. The genetic observation of *p53* dependence does not distinguish between reliance and modulation.

Using RNAi, gene knockouts, and double knockouts to strip away particular paths and regulators showed that the entire effect of UV-induced P53 on down-regulating Bcl-2 is mediated through E2f1, and virtually all of P53–E2f1's regulation of the direct UVB apoptosis pathway proceeds through Bcl-2 (Figs. 2 and 3). The level of UVB-induced apoptosis in the $p53^{-/-}$;$E2f1^{-/-}$ double knockout (which lacks P53-induced Bax, Bak, Puma, PIGs, Noxa, and P53's direct binding to proteins at the mitochondrion) was equal to apoptosis in wild type, so P53's action in disinhibiting the direct pathway equals or exceeds that of its traditional proapoptotic effectors. A quantitative accounting of the percentage contribution of various pathways is important for understanding the network.

Secondary Effects. Engineering and physics commonly distinguish between the primary effects in a system and smaller, secondary effects. Here two secondary pathways are present whose effects become observable only when the basal level of Bcl-2 is low, as it is in $E2f1^{-/-}$ cells. First, P53 moderately stimulates Bcl-2 (Fig. 2 *C* and *D*). Under normal conditions, however, this pathway is overwhelmed by the P53–E2f1 inhibitory pathway (e.g., losing *p53* in $E2f1^{+/+}$ cells causes at most a 10% drop in Bcl-2) (Fig. 2*A*). Despite this lower basal Bcl-2 level in the E2f1 knockout, nonirradiated E2f1 knockout cells do not undergo spontaneous apoptosis. The cells have clearly adjusted to compensate for low basal Bcl-2. This fact means that it is the UV-induced changes in the levels of apoptosis proteins, rather than absolute levels, that trigger UV-induced apoptosis.

Second, UVB has a modest inhibitory effect on Bcl-2 that is independent of E2f1. This pathway is revealed by photoreactivation in $p53^{-/-}$;$E2f1^{-/-}$ cells (Fig. 4). Yet it scarcely reduces Bcl-2 in $E2f1^{-/-}$ single-knockout cells (Fig. 2*A*): In these cells, both secondary pathways are present and approximately cancel each other, so that Bcl-2 remains approximately constant after UVB irradiation (Figs. 2*A* and control lanes of 3*D*). UVB induces apoptosis nevertheless: Because Bcl-2 is already low in $E2f1^{+/+}$ cells, the direct pathway does not need to be disinhibited by P53.

A UV Signaling Node at Bcl-2. The UVB inputs to the UV-apoptosis switch, Bcl-2, and direct pathway fit an emerging theme in biological networks: The same input acts at multiple points. Here UVB acts at five points: Four converge on Bcl-2, and one triggers a pathway that Bcl-2 then inhibits (Fig. 5). Focusing on the biochemistry of individual proteins cannot show the interaction of pathways or the switch behavior of the network. A hallway light that can be turned on at either end of the hall cannot be understood by studying how a toggle handle works. Conversely, Bayesian computational approaches to complex networks require that all of the members be known; moreover, these approaches typically ignore feedback loops due to computational limitations (10).

The three signals through P53 and Mdm2 arise from DNA photoproducts in actively transcribed genes (23, 26, 27). Normal P53 protein is then up-regulated (28) by increased protein translation rate and decreased Mdm2-mediated protein turnover; the P53–Mdm2 loop has its own network behavior (29). The fourth Bcl-2 signal also arises from nucleic acid photoproducts and proceeds by a non-P53–E2f1 route to inhibit Bcl-2. The initiating photoproducts for this pathway are most likely in nuclear DNA because only photolyases from higher plants are known to be active on RNA (24), and motif analysis indicates that the protein targeting sequence of the *Anacystis nidulans* photolyase used here is unlikely to direct the protein to mitochondria (D. Brown, personal communication). The direct pathway may include downstream targets of Bcl-2. Entry points for Jnk (18) and signals from receptor kinases (30) remain to be identified.

Materials and Methods

Primary Skin Fibroblasts and UV Irradiation. $p53^{-/-}$;$E2f1^{-/-}$ mice and matched wild-type and single-knockout controls were generated by mating (3), and primary newborn fibroblasts were prepared (31) by using protocols approved by the Yale Institu-

tional Animal Care and Use Committee. Cells at passage <5 were grown in DMEM high-glucose medium, rinsed with saline, and exposed to predominantly UVB (3) at physiological doses (≤50% apoptosis, corresponding to ≤12 J/m^2 UVC *in vitro*).

RNAi and Vector Transfection. RNAis were from Dharmacon (Lafayette, CO) using their RNAi design center. siControl contains at least four mismatches with all known human, mouse, and rat genes. Primary murine fibroblasts were plated at <50% confluency (300,000 cells per 60-mm plate) 16 to 20 h before transfection in penicillin/streptomycin-free medium at a ratio of 6:1 (vol:vol) Oligofectamine (Invitrogen, Carlsbad, CA) to RNAi and incubated with cells in Opti-MEM low-serum medium (Gibco BRL, Carlsbad, CA) for 5 to 6 h per the manufacturer's instructions. Expression vector pUSE-Bcl-2 was from Upstate Biotechnology (Waltham, MA). pCMV-p53 (32) and pcDNA3.1-E2F1 (33) were generous gifts of R. Reddel (Children's Medical Research Institute, Westmeade, Australia) and R. Halaban (Yale University). Lipofectamine 2000 reagent (Invitrogen) in Opti-MEM was used at a ratio of 5:1 to vector DNA per manufacturer's instructions, incubated for 4 h at 37°C, and washed. RNAi inactivation or vector expression occurred in 24 to 48 h.

Apoptosis and Immunoblots. Approximately 200,000 trypsinized cells were assessed for apoptosis 20 h after UVB irradiation by using the Vybrant 3 Annexin V/propidium iodide apoptosis kit (Molecular Probes, Eugene, OR) as described (3). Immunoblot antibodies were from Santa Cruz Biotechnology (Santa Cruz, CA). Secondary antibody was visualized by using supersignal substrate (Pierce, Rockford, IL) and ECL film (Amersham, Piscataway, NJ), which produce linear signals proportional to the antibody binding. Films were scanned (Hewlett Packard, Palo Alto, CA) and TIFF files imported into ImageJ software to calculate band intensity above background. Repeated experiments were averaged. Error bars represent standard deviation, and statistical significance of differences was determined by using the two-tailed heteroscadastic Student's *t* test.

Photolyase. Liposomes containing *A. nidulans* photolyase (Photosomes, AGI Dermatics, Freeport, NY) were used by modifying a standard protocol (25). After 1 h of photosome preincubation, cells were irradiated with 750 J/m^2 UVB to create cyclobutane dimers and other DNA photoproducts, followed by 12,000 J/m^2 UVA from eight F20T12BL lamps (Spectra Mini; Daavlin, Bryan, OH) to allow photolyase molecules to monomerize cyclobutane dimers to which they have bound; room light at the time of cell harvesting can also contribute. UVA was passed through an 11-mm plate glass filter to remove UVB and UVC; duration of UVA exposure was ≈5 min.

We thank A. Diaz and V. Pham for experimental assistance, Drs. D. Yarosh and D. Brown (AGI Dermatics, Inc., Freeport, NY) for photosomes and protein-targeting sequence analysis of the *A. nidulans* photolyase gene, and R. Carbone for assistance with FACS analysis. This work was supported by National Cancer Institute Grant CA55737 (to D.E.B.) and an Anna Fuller Fund predoctoral fellowship (to D.K.).

1. Vousden KH, Lu X (2002) *Nat Rev Cancer* 2:594–604.
2. Chipuk JE, Bouchier-Hayes L, Green DR (2006) *Cell Death Differ* 13:1396–1402.
3. Wikonkal NM, Remenyik E, Knezevic D, Zhang W, Liu M, Zhou H, Berton TR, Johnson DG, Brash DE (2003) *Nat Cell Biol* 5:655–660.
4. Berton T, Mitchell D, Guo R, Johnson D (2005) *Oncogene* 24:2449–2460.
5. Shan B, Lee WH (1994) *Mol Cell Biol* 14:8166–8173.
6. Wu X, Levine AJ (1994) *Proc Natl Acad Sci USA* 91:3602–3606.
7. Qin XQ, Livingston DM, Kaelin WGJ, Adams PD (1994) *Proc Natl Acad Sci USA* 91:10918–10922.
8. Stevens C, La Thangue NB (2004) *DNA Repair (Amst)* 3:1071–1079.
9. Kowalik TF, DeGregori J, Schwarz JK, Nevins JR (1995) *J Virol* 69:2491–2500.
10. Knezevic D, Brash DE (2004)) *Cell Cycle* 3:729–732.
11. Nevins JR (1998) *Cell Growth Differ* 9:585–593.
12. Phillips AC, Vousden KH (2001) *Apoptosis* 6:173–182.
13. Ma Y, Croxton R, Moorer RL, Cress WD (2002) *Arch Biochem Biophys* 399:212–224.
14. Danno K, Horio T (1987) *Photochem Photobiol* 45:683–690.
15. Orren DK, Petersen LN, Bohr VA (1995) *Mol Cell Biol* 15:3722–3730.
16. McKay B, Becerril C, Spronck J, Ljungman M (2002) *DNA Repair (Amst)* 1:811–820.
17. Ziegler A, Jonason AS, Leffell DJ, Simon JA, Sharma HW, Kimmelman J, Remington L, Jacks T, Brash DE (1994) *Nature* 372:773–776.
18. Tournier C, Hess P, Yang DD, Xu J, Turner TK, Nimnual A, Bar-Sagi D, Jones SN, Flavell RA, Davis RJ (2000) *Science* 288:870–874.
19. Washio F, Ueda M, Ito A, Ichihashi M (1999) *Br J Dermatol* 140:1031–1037.
20. Breitschopf K, Haendeler J, Malchow P, Zeiher AM, Dimmeler S (2000) *Mol Cell Biol* 20:1886–1896.
21. Dunkern TR, Fritz G, Kaina B (2001) *Oncogene* 20:6026–6038.
22. Naik E, Michalak EM, Villunger A, Adams JM, Strasser A (2007) *J Cell Biol* 176:415–424.
23. Brash DE, Wikonkal NM, Remenyik E, van der Horst GTJ, Friedberg EC, Cheo DL, van Steeg H, Westerman A, van Kranen HJ (2001) *J Invest Dermatol* 117:1234–1240.
24. Harm W (1980) *Biological Effects of Ultraviolet Radiation* (Cambridge Univ Press, Cambridge, UK).
25. Kulms D, Poppelmann B, Yarosh D, Luger TA, Krutmann J, Schwarz T (1999) *Proc Natl Acad Sci USA* 96:7974–7979.
26. Yamaizumi M, Sugano T (1994) *Oncogene* 9:2775–2784.
27. Ljungman M, Zhang F (1996) *Oncogene* 13:823–831.
28. Maltzman W, Czyzyk L (1984) *Mol Cell Biol* 4:1689–1694.
29. Bar-Or RL, Maya R, Segel LA, Alon U, Levine AJ, Oren M (2000) *Proc Natl Acad Sci USA* 97:11250–11255.
30. Kamata H, Honda S, Maeda S, Chang L, Hirata H, Karin M (2005) *Cell* 120:649–661.
31. Hager B, Bickenbach J, Fleckman P (1999) *J Invest Dermatol* 112:971–976.
32. Noble JR, Willetts KE, Mercer WE, Reddel RR (1992) *Exp Cell Res* 203:297–304.
33. Cress WD, Johnson DJ, Nevins JR (1993) *Mol Cell Biol* 13:6314–6325.